THE JOURNAL OF PHYSICAL CHEMISTRY A

ARTICLE

pubs.acs.org/JPCA

Heterogeneity in Binary Mixtures of (Water + Tertiary Butanol): Temperature Dependence Across Mixture Composition

Harun Al Rasid Gazi and Ranjit Biswas*

Department of Chemical, Biological & Macromolecular Sciences, S. N. Bose National Centre for Basic Sciences, JD Block, Sector III, Salt Lake, Kolkata 700 098, India

Supporting Information

ABSTRACT: The temperature dependence of solution heterogeneity in binary mixtures of water and tertiary butanol (TBA) and its effects on a chemical reaction have been investigated by using steady-state and time-resolved spectroscopic experiments within the temperature range of 278 ≤ T/K ≤ 373. Eleven different mole fractions of TBA, covering extremely low TBA mole fractions to pure TBA, have been considered. An organic chromophore that undergoes a photoexcited intramolecular charge-transfer reaction is employed to reveal the signature of the solution heterogeneity. Upon increasing the solution temperature, the absorption spectrum of the dissolved chromophore exhibits a red shift at very low TBA concentrations but shifts toward higher energy (blue shift) at higher alcohol concentrations. This is a reflection of temperature-assisted aggregation of TBA molecules in very dilute aqueous solutions. The magnitude of the temperature-induced red shift is the largest at around 0.04 mol fraction of TBA, and a larger variation of the spectral line width across the temperature suggests enhanced solution heterogeneity. Reaction time constants measured at various mixture compositions are found to follow an Arrhenius-type temperature dependence. The average activation energy, when plotted as a function of mixture composition, steeply rises with TBA concentration in the limit of the very low TBA mole fraction and then suddenly levels off to a plateau upon further addition of TBA. The alcohol concentration-dependent activation energy abruptly changes its slope at a TBA mole fraction ∼0.1, at which a transition from the three-dimensional water-type network to the zigzag alcohol chain structure is known to occur. The plateau value of the activation energy is ∼6k_BT and agrees well with the earlier estimate for the same chromophore from the pure solvent data at room temperature. The observed increase in the spectral red shift with temperature at low TBA mole fractions is in general agreement with the existing experimental results which support the view that temperature assists the aggregation of TBA molecules in dilute aqueous solutions of TBA. However, unlike in the small-angle neutron scattering study [Bowron, D. T.; Finney, J. L. J. Phys. Chem. B 2007, 111, 9838], which finds clustering of TBA molecules reaching a maximum at ∼353 K, the present data do not indicate any such temperature maximum within the temperature range of 278 ≤ T/K ≤ 373.

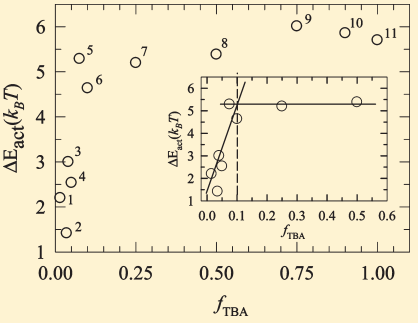

1. INTRODUCTION

Microscopic heterogeneity in aqueous alcoholic solutions has been known for a long time and has been revealed by neutron diffraction,[1−3] small-angle X-ray scattering,[4−6] light scattering,[4,7−9] and other experimental and simulation studies.[10−15] Tertiary butanol (TBA) is an amphiphile that possesses both hydrophobic and hydrophilic moieties in the same molecule. Consequently, TBA can participate in both hydrophobic and hydrophilic interactions with water via its tertiary butyl (−CMe_3, Me = CH_3) and hydroxyl (−OH) groups respectively, leading to segregation of aqueous solutions into microscopic polar and nonpolar domains.[16] This is reflected in the anomalous change in several thermodynamic properties. While clustering of TBA molecules via interactions among the −CMe_3groups creates the nonpolar domains of a few molecules to several tens of molecules,[17] participation of alcoholic −OH groups in hydrogen bonding (H-bonding) with neighboring water molecules leads to the formation of polar zones. The microscopic phase segregation due to clustering is the strongest at a TBA mole fraction (f_{TBA}) near 0.04. At lower mole fraction of TBA, strengthening of the H-bonding network is believed to occur due to accommodation of TBA molecules in the water network,[18] where the latter (the water network) simply go around the hydrophobic group.[19] A transition from the tetrahedral-like water structure at lower f_{TBA} to the typical zigzag chain structure of alcohol appears at $f_{TBA} \approx 0.1$, which remains so until the medium becomes pure TBA.[17,18,20−22]

Interestingly, the hydrophobic interaction that drives the aggregation of small nonpolar solutes and amphiphilic molecules in dilute aqueous solutions[23−28] has been found to increase with increasing temperature.[8,9,22,29−36] Recent small-angle neutron scattering (SANS) experiments with 0.04 mol fraction TBA solution in water[17] have indicated that the TBA clustering reaches the maximum at ∼353 K. The increase in clustering

Received: October 12, 2010
Revised: February 12, 2011
Published: March 03, 2011

with temperature is believed to originate from the increase in entropy as a few water molecules are released in the bulk when two hydrophobic surfaces come into contact.[19] Therefore, the clustering process is entropy-driven where the water structure is disrupted and the subsequent dehydration lowers the free energy of the solution. Further increase in temperature leads to partial declustering as hydration of relatively smaller clusters wins over the dehydration.[32,33,37] Unfortunately however, temperature-dependent experimental measurements for a wide range of TBA mole fractions are not available. Significant temperature dependence at higher alcohol concentrations ($f_{TBA} > 0.1$) is probably not expected as cluster growth via dehydration of solvent-separated smaller clusters may not lead to substantial free-energy gain in this regime. In fact, determination of concentration-dependent excess partial molar activation free energy at room temperature from the dielectric relaxation measurements with the ethanol−water system,[38] a system that also shows solution structural transition at $f_{EtOH} \approx 0.2$ and strong hydrophobic hydration, has indicated negligible or no free-energy gain in aqueous solutions with $f_{EtOH} \geq 0.2$. This study has also suggested that in solutions with $f_{EtOH} \geq 0.2$, ethanol molecules are in the same environment as those in pure alcohol, existing as chainlike clusters surrounded or exothermically attached to water molecules via H-bonding.

In this paper, we explore the temperature dependence of the microscopic heterogeneity in water−TBA mixtures in the temperature range of $278 \leq T/K \leq 373$ at 11 different TBA concentrations, starting from an extremely dilute solution ($f_{TBA} = 0.015$) to pure TBA ($f_{TBA} = 1$). Here, we use the excited-state intramolecular charge-transfer (ICT) reaction as a probe for the inherent solution heterogeneity. Note that our earlier study of ICT reaction in water−TBA mixtures at room temperature has shown considerable effects of solution heterogeneity on both the reaction equilibrium and time constants.[10] Subsequent fluorescence anisotropy studies with a nonreactive dipolar probe in water−TBA and water−ethanol mixtures[11] have revealed a solution structural transition by showing an abrupt change in the slopes of the alcohol concentration dependence of the solute rotation time at $f_{TBA} \approx 0.10$ and $f_{EtOH} \approx 0.2$. Even though absorption and fluorescence spectroscopy cannot provide the length scale of the solution heterogeneity, steady-state spectral response can very well reflect the change in the average local environment around a dissolved solute via the spectral shift and width. If the solute also undergoes photoinduced reaction in solution, any modification of the environment−solute coupling is further revealed in the reaction equilibrium and time constants. This information of solute−medium coupling via monitoring the steady-state and time-resolved spectroscopic signatures is then utilized to understand the solution heterogeneity and its temperature dependence in water−TBA solutions at various mixture compositions.

We have chosen 4-(1-azetidinyl) benzonitrile (P4C) as a solute molecule that undergoes a photoinduced excited-state intramolecular charge-transfer reaction. Upon photoexcitation in polar solvent, P4C undergoes conversion from the locally excited (LE) state to the more polar charge-transferred (CT) state and shows dual fluorescence because of the emissive nature of both the LE and CT states.[39] The reaction barrier (ΔG^*) involved in the excited-state LE → CT conversion reaction in P4C is $\sim 6k_BT$, which has been found to be strongly dependent on the medium polarity but insensitive to the dynamics of it.[39] The photoconversion reaction of P4C and its analogues has already been studied in diverse media,[10,11,40−44] and the kinetics have been described reasonably well in terms of the twisted intramolecular charge-transfer (TICT) model.[45,46] Scheme 1 depicts the TICT reaction mechanism and the related kinetics. The TICT model is also employed here to analyze the experimental data, even though alternative models[47,48] exist in the relevant literature. Within such a two-state model and in the assumed rapid reaction equilibration limit, the time-dependent fluorescence intensity has been shown to be biexponential. Indeed, a biexponential function with short (τ_{short}) and long (τ_{long}) time constants has been found to sufficiently describe the decay kinetics of P4C at all TBA concentrations and temperatures considered here. In contrast, the intensity decay in a nonpolar solvent like heptane is monoexponential with only the long time constant, regardless of the collection wavelength across the structureless emission spectrum of P4C in this solvent. τ_{short} is therefore ascribed to the reaction time constant ($\tau_{short} \equiv \tau_{rxn} = k_{rxn}^{-1}$, k_{rxn} being the rate constant) and τ_{long} to the average LE or CT lifetime.

Scheme 1. (A) Photoinduced Charge Transfer and Simultaneous Twisting of the Donor Group around the Central Bond Joining the Benzonitrile Moiety (acceptor) within the TICT Model and (B) Various Rate Processes Associated with the Reaction within the above Model

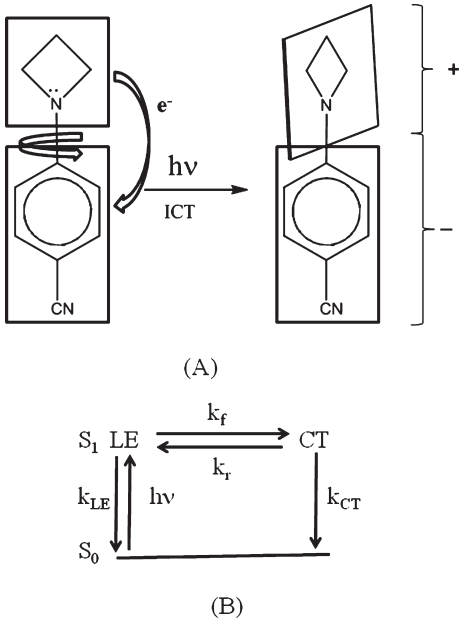

The rest of the paper is organized as follows. Experimental details are given in the next section. Section 3 contains experimental results, analyses of which are based on equations derived in ref 39. The paper finally ends with concluding remarks in section 4.

2. EXPERIMENTAL SECTION

Synthesis of P4C was carried out by following the literature method[49,50] and recrystallization twice from cyclohexane (Merck, Germany). The presence of impurity was checked by thin-layer chromatography and also by monitoring the excitation wavelength dependence of the fluorescence emission (for fluorescent impurity). TBA was obtained from Aldrich and used without further purification. Deionized water (Millipore) was

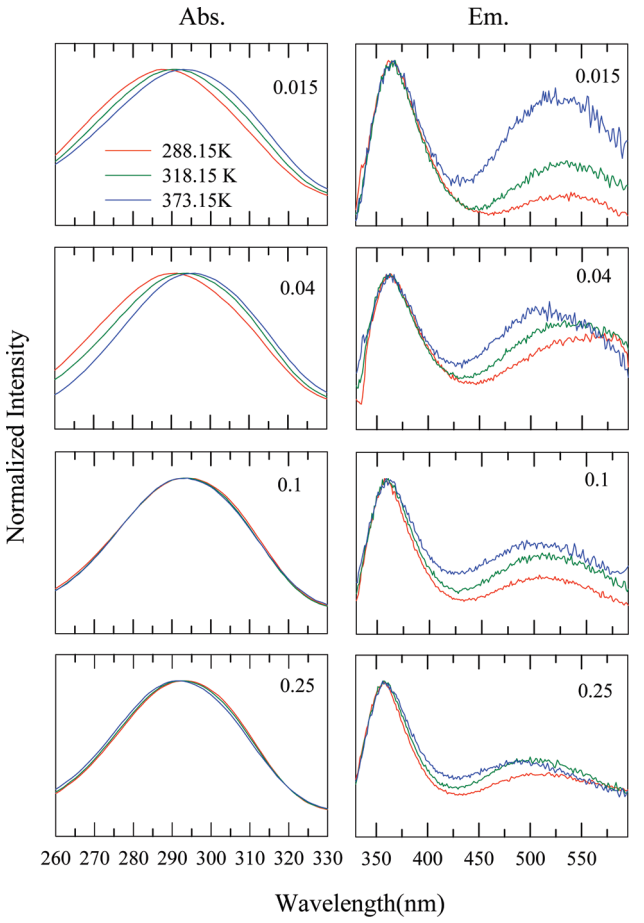

Figure 1. Temperature-dependent absorption (left panels) and emission spectra (right panels) of 4-(1-azetidinyl)benzonitrile (P4C) in water−TBA binary mixtures at four different TBA mole fractions, − 0.015, 0.04, 0.1, and 0.25. Spectra at different temperatures are color-coded and shown as a function of wavelength.

used for preparing stock solutions at different TBA mole fractions. Subsequently, a freshly prepared 5 μL solution of P4C in heptane of known concentration was transferred into a quartz cuvette (optical path length 1 cm), and the nonpolar solvent was evaporated off completely by gently blowing dry N_2 gas into it. An aliquot of the stock water−TBA solution was then transferred into the cuvette in such a way that the concentration of P4C was maintained at $\leq 10^{-5}$ M in all TBA mole fractions studied here. The solution in the cuvette was then shaken very well, temperature equilibrated (Julabo), and the absorption spectrum was recorded using a UV−visible spectrophotometer (Shimadzu, UV-2450). Corrected fluorescence emission spectra were collected by using a fluorimeter (Fluoromax-3, Jobin-Yvon) whose sample chamber was pre-equilibrated at the desired temperature. The temperature of sample chamber was varied from ∼278 to ∼373 K (±0.5 K). For steady-state emission collection, the excitation wavelength was fixed at 300 nm for all measurements. Solvent blanks were subtracted from the emission spectra prior to analysis and converted to frequency representation after properly weighting the intensity with λ^2.

Shifts of the absorption spectra from the peak of the reference absorption spectra were determined and added to the average peak frequency of the absorption spectra to obtain the absorption peak frequencies. The average of the reference absorption peak frequency was calculated by averaging the numbers obtained by fitting the upper half of the reference absorption spectrum with an inverted parabola, the first moment, and the arithmetic mean of the frequencies at half intensities on both the blue and red ends of the absorption spectrum.[51,52] The error associated with the peak frequency determination is typically ±250 cm^{-1}, unless otherwise mentioned. The time-correlated single-photon counting (TCSPC) technique based on a laser system (Lifespec-ps, Edinburgh, U.K.) with a light-emitting diode (LED) was used to collect fluorescence emission intensity decays. The excitation wavelength was 299 nm, and the full width at half-maximum (fwhm) of the instrument response function (IRF) was ∼475 ps. Emission decays were collected at both LE and CT peak positions (of the steady-state spectrum) with an emission band-pass of 8 nm at the magic angle to avoid effects of solute rotation.[53] Subsequently, the collected emission decays were deconvoluted from the IRF and fitted to biexponential functions of time using an iterative reconvolution algorithm.[54] Such an iterative process is believed to be capable of describing dynamical events approximately 3−5 times faster than the fwhm of the IRF.[55,56] Biexponential fit to each of the collected LE emission decays produced one short time constant and one long time constant, whereas each of the CT emission decay (collected wherever possible) fits generated one rise time (similar to the short time constant of LE decay) and one long time constant. This observation further supported the assignment of the short time constant as the reaction time constant (or the inverse of the reaction rate constant). For a few cases, emission decays were collected at two or three different emission wavelengths around the LE and CT peaks, and the analyzed data were found to vary within a small uncertainty.

3. RESULTS AND DISCUSSION

A. Steady-State Studies. Temperature-dependent absorption and emission spectra of P4C in TBA−water solutions at f_{TBA}= 0.015, 0.04, 0.1, and 0.25 are shown in Figure 1. It is interesting to note in Figure 1 (also Figure S1, Supporting Information) that a rise in temperature gives rise to a red shift in the absorption spectrum of P4C in water−TBA mixtures at $f_{TBA} < 0.1$, but at higher TBA mole fractions ($f_{TBA} \geq 0.1$), the same temperature rise induces a blue shift. This temperature-induced red shift of the absorption spectrum in solutions with $f_{TBA} < 0.1$ and the blue shift at $f_{TBA} \geq 0.1$ can be understood from the solute aggregation in water−TBA mixtures, which depends on both the solution temperature and alcohol concentration.[8,9,17,22,35,36] The well-known temperature-assisted growth of the cluster (or nonpolar domain) drives the expelled water molecules near the alcoholic hydroxyl groups so that the H-bonding constraints are satisfied. This, in turn, leads to the temperature-induced enhancement of the local polarity of the microscopic polar domains. P4C, being a polar solute, would naturally prefer to reside more in such domains of enhanced polarity. The observed red shift in the absorption spectrum is, therefore, a reflection of the enhanced polarity of these microscopic domains formed due to the increased hydrophobic effects at higher temperatures in solutions containing very low mole fractions of TBA. As f_{TBA} approaches 0.1, solution structural transition occurs, affecting strongly the extent of aggregation. This leads to a reduction in the size of such domains with enhanced polarity upon an increase in the temperature. As a result, the spectrum starts moving in the opposite direction. At

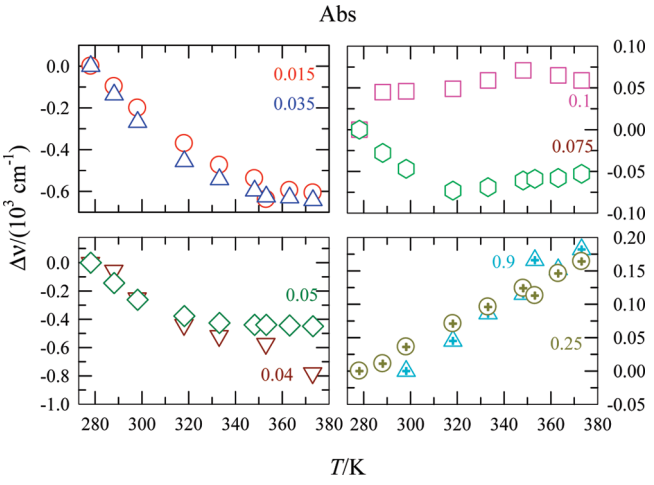

Figure 2. Temperature-dependent relative absorption shift at 0.015 and 0.035 (left upper panel), 0.04 and 0.05 (left lower panel), 0.075 and 0.1 (right upper panel), and 0.25 and 0.9 (right lower panel). The color of the temperature-dependent shift values correspond to that of the TBA mole fractions shown in each of the panels. Repeat experiments at a few TBA mole fractions and temperatures indicate a maximum error of ±7% associated with these shift values. For a definition of the relative absorption shift, please see the text.

$f_{TBA} \geq 0.1$, blue shift occurs because the absorption transition energy at these mole fractions is now determined mainly by the temperature-dependent average polarity of the aqueous mixture.[15] Interestingly, the fluorescence emission spectrum exhibits only a blue shift with the rise in the solution temperature. It was already discussed in our earlier work[10] that the environment around a photoexcited solute can undergo many fluctuations during its lifetime (~1 ns or longer) due to a much shorter stability time (a few tens of picoseconds)[57] of these clusters, and thus, the fluorescence emission is governed only by the average polarity of the solution. Because successive addition of TBA reduces the static dielectric constant (ε_0) of the aqueous mixture and because the rise in temperature also decreases the individual ε_0 of both water ($\varepsilon_0 \approx 78$)[58,59] and TBA ($\varepsilon_0 \approx 12$),[60,61] the emission spectrum shifts to higher frequency upon increasing either the alcohol concentration or the solution temperature.

The fact that temperature affects the aggregation process differently at different alcohol mole fractions is shown more quantitatively in Figure 2, where the relative absorption shifts for various f_{TBA} values are shown as a function of temperature. The temperature-dependent relative absorption shift (in proper unit) is defined as $\Delta\nu_{Abs.} = \nu_{Abs.}(f_{TBA},T) - \nu_{Abs.}(f_{TBA},T_{Lowest})$, where $\nu_{Abs.}(f_{TBA},T)$ denotes the peak frequency of the absorption spectrum at any TBA mole fraction and temperature and $\nu_{Abs.}(f_{TBA},T_{Lowest})$ the frequency at that alcohol concentration but at the lowest temperature accessible. Therefore, negative and positive values of $\Delta\nu_{Abs.}$ denote, respectively, the temperature-dependent red and blue shifts of the absorption spectrum with respect to that at the lowest temperature accessible at that mixture composition. Figure 2 clearly demonstrates that the rise in solution temperature increasingly assists the aggregation process at very low f_{TBA} values as $\Delta\nu_{Abs.}$ becomes more negative with temperature in this limit. In fact, the total red shift between the absorption spectra at the highest and lowest temperatures (373 and 278 K) is ~800 cm^{-1} at $f_{TBA} \approx 0.04$, which is the maximum among those measured at f_{TBA} values of 0.015, 0.035, 0.04, 0.05, and 0.075. This suggests that the stronger clustering tendency at the 0.04 mol fraction of TBA near room temperature is preserved for a fairly broad range of temperature change. These shift data, other than this mole fraction maximum, do not indicate any temperature maximum for aggregation within the temperature range considered. Interestingly, SANS experiments with aqueous solutions at $f_{TBA} = 0.04$ have revealed[17] that the cluster size increases with temperature and finally becomes the maximum at ~353 K. Available light-scattering[8,9,22] and small-angle X-ray scattering (SAXS)[35] data for dilute aqueous solutions of TBA also suggest an increase in cluster size with temperature in the range of $273 \leq T/K \leq 345$. The nonobservation of a temperature maximum of the shift in very dilute solutions is therefore counterintuitive as deaggregation at further higher temperatures and prominence of solvent-separated smaller clusters are expected due to enthalpy effects. However, SANS measurements of a TBA-rich aqueous solution at ~298 K in the presence of a third nonpolar component, cyclohexene, have revealed[3] much less microscopic phase segregation relative to that in binary TBA−water mixtures. The improved homogeneous solution structure is then explained in terms of a better packing of the alcohol methyl groups in the presence of the nonpolar third component and increased alcohol−alcohol H-bonding interactions. The chromophore (P4C) used here is sparingly soluble in water, and thus P4C, like cyclohexene in SANS measurements,[3] may induce more efficient packing of TBA molecules in this low concentration regime as well. This more compactness and the increased solution homogeneity probably inhibit deaggregation in a ternary solution beyond a certain temperature, forcing a near constancy in the spectral shift value at higher temperatures in the very low TBA concentration regime. Temperature-dependent SANS measurements of this kind of ternary mixtures are therefore required to further understand how various interactions are resolved in such complex systems even though the shift data presented in Figure 2 are in general agreement with the existing experimental results[2,8,9,17,35] and computer simulations.[32,33]

Data presented in Figure 2 suggest that the total red shift decreases by a factor of ~5 as f_{TBA} increases from 0.05 to 0.075 and signal a transition in solution structure as the blue shift appears at $f_{TBA} = 0.1$. However, the highest total blue shift observed is ~250 cm^{-1} (see also Figure S2, Supporting Information), which is ~4 times less than the highest red shift observed at very low TBA mole fractions. Because the temperature dependence of ε_0 for monohydroxy alcohols is much weaker[58] than that for water,[57] it is probably not unexpected that the magnitude of the blue shift would vary within a narrow range for solutions rich in TBA. What is remarkable is that at very low TBA mole fractions where ε_0 is expected to decrease rather sharply with temperature, the effects of the temperature-induced decrease of the average solution polarity (on the spectral shift) is overwhelmed by the effects of temperature-assisted aggregation in solution. Spectral widths (fwhm) presented in Table S3 (Supporting Information) reveal that changes in width at a given mixture composition across the temperature are smaller than the total spectral shift. This suggests that the observed spectral shifts are indeed deriving contributions from the physical movement of the spectrum with temperature. More interestingly, the range (~250−550 cm^{-1}) over which the spectral width varies across the temperature in very dilute TBA solutions ($f_{TBA} < 0.1$) is much larger than that (40−80 cm^{-1}) at higher TBA mole fractions. This provides further support in favor of a transition

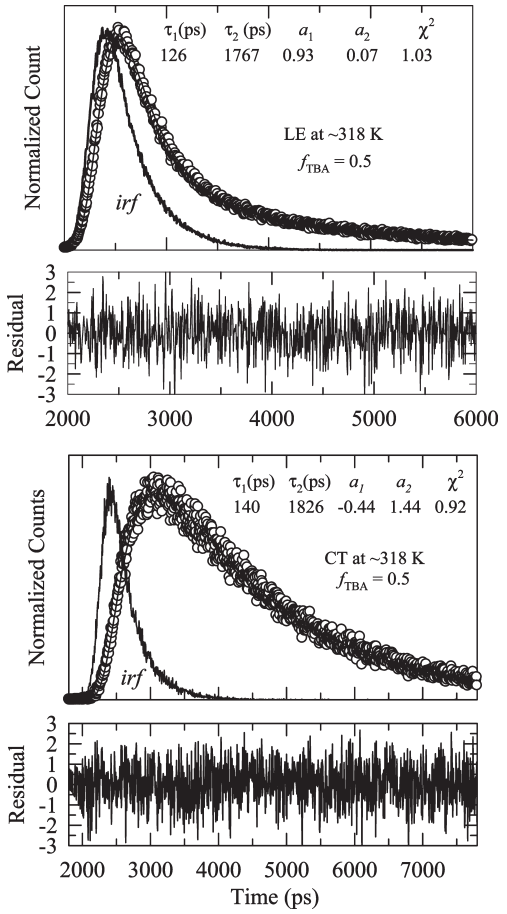

Figure 3. Representative LE (upper panels) and CT (lower panels) emission decays of P4C in water−TBA mixtures at a 0.5 TBA mole fraction. While the data are represented by the circles, fits through the data are denoted by solid lines. The instrument response function is also shown and indicated. Corresponding biexponential fit parameters are provided in both panels.

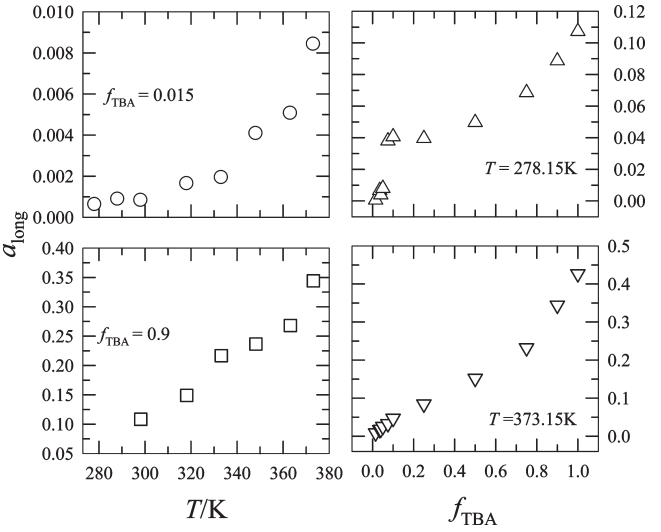

Figure 4. Temperature and solution composition dependence of the component (a_{long}) associated with the longer of the two time constants obtained from biexponential fits. While the temperature dependence of a_{long} at two extreme values of TBA mole fractions are shown in the left panels, the TBA mole fraction dependence of it (a_{long}) at two extreme temperatures is presented in the right panels. The values of representative TBA mole fractions and temperatures are indicated in respective panels. The amplitudes shown here are better than ±10% uncertainty about their numerical values (based on limited repeat experiments).

from a heterogeneous solution structure at very low TBA mole fractions to a relatively more homogeneous one at higher alcohol contents.

B. Time-Resolved Fluorescence Emission Studies. Time-resolved emission decays of P4C at 11 different TBA mole fractions have been collected by varying the solution temperature within the range of $278 \leq T/K \leq 373$ in order to explore the temperature dependence of heterogeneity effects on the rate of LE → CT conversion reaction in this molecule. As already observed earlier, all of the collected emission decays have been found to be biexponential with time at all TBA mole fractions. This is somewhat counterintuitive in the sense that one would expect a stretched exponential[62,63] rather than a simple biexponential decay at least in those mixture compositions and temperatures where microscopic heterogeneity governs the solution structure. However, biexponential kinetics may originate either from the rapid fluctuations in the immediate environment of the photoexcited P4C due to the relatively faster lifetime of the TBA clusters or from the inability of the present experiments to detect the faster decay components due to the insufficient time resolution employed.

Representative unconstrained biexponential fits to the emission decays collected at peak wavelengths of LE and CT bands of P4C in aqueous solution with $f_{TBA} = 0.5$ at ∼318 K are shown in Figure 3 along with fit parameters and residuals. It is evident from Figure 3 that biexponential functions adequately describe both the LE and CT emission decays as the residuals do not contain any nonrandom pattern[64] and values for the goodness of fit parameter (χ^2) are close to 1. Fit parameters shown in the panels also indicate that the unconstrained fits produce very similar time constants for the fast LE decay (126 ps) and CT rise (140 ps). This similarity in short time constants suggests that the faster one of the two time constants obtained from biexponential fit to either LE or CT emission intensity decay corresponds to the reaction time constant ($\tau_{short} \equiv \tau_{rxn} = k_{rxn}^{-1}$, k_{rxn} being the reaction rate constant) associated with the LE → CT conversion reaction in aqueous TBA solutions. Similar behavior has been observed for other collected emission decays as well, and this simplifies the interpretation of the temperature dependence of the reaction time constant in aqueous solutions at various mixture compositions. Therefore, the biexponential behavior of the decay kinetics for P4C in water−TBA mixtures at all temperatures (within the range studied) also conforms to the classical two-state reversible reaction mechanism as found in several earlier studies.[39−44] However, with the long time component ($a_{long} \equiv a_2$) being so tiny, one wonders whether a component of such an insignificant amplitude is at all required to fit the LE emission decay. Figure S4 (Supporting Information) demonstrates that noninclusion of this insignificant component in the fit produces an unacceptable pattern of the residual and a large value of χ^2. This clearly indicates that a slow component (a_{long}), however small it may be, is required to properly describe the LE emission intensity decays. In addition, the presence of the LE emission band in the steady-state fluorescence emission spectra at all TBA mole fractions further ensures the presence of such a component in the time-resolved LE emission decays.

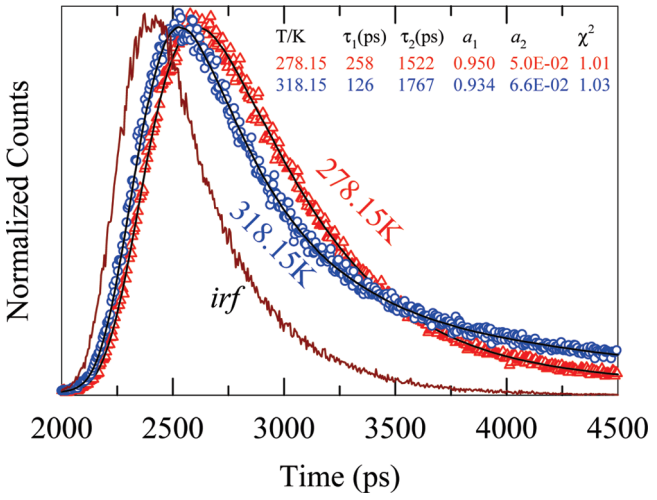

Figure 5. Temperature dependence of the LE → CT conversion reaction of P4C in an aqueous solution of TBA at f_{TBA} = 0.5. Red triangles represent the collected decay at ~278 K, blue circles represent the decay at ~318 K, and the solid black lines denote the biexponential fits through the experimental decays. Biexponential fit parameters are shown inside of the panel.

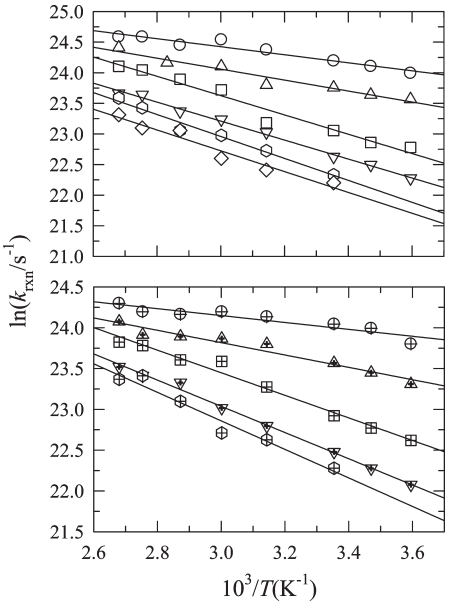

Figure 6. Arrhenius temperature dependence of the reaction rate constant. The natural logarithms of the reaction rate constant (k_{rxn} = τ_{rxn}^{-1}) at various solution compositions are shown as a function of inverse temperature. The data representations are as follows: circles, triangles, squares, inverted triangles, hexagons, and diamonds in upper panel denote TBA mole fractions 0.015, 0.04, 0.075, 0.25, 0.75 and 1.0, respectively. Circles crossed, triangles crossed, squares crossed, inverted triangles crossed, and hexagons crossed show data for aqueous solutions at TBA mole fractions 0.035, 0.05, 0.1, 0.5 and 0.9, respectively. Lines going through the points represent linear fits to the natural logarithm of the temperature-dependent rate constant expressed by the Arrhenius equation discussed in the text. On the basis of limited repeat experiments, the maximum error associated with the rate constant values has been found to lie within ±10% (of the reported values).

The variations of this long time component with mixture composition and temperature are further explored in Figure 4, where the temperature dependence of a_{long} at two extreme values of f_{TBA} and the TBA mole fraction dependence of it (a_{long}) at two extreme temperatures are presented. This figure shows that a_{long} is quite small (even vanishingly small in some cases) and increases as either the solution temperature is raised or alcohol added in the solution. A rise in the solution temperature reduces the ε_0 of these associative solvents (water and TBA), and as a result, formation of CT population is increasingly suppressed at higher temperatures. This, in turn, enhances the relative LE population as the temperature is increased. Successive addition of TBA at a given temperature increases a_{long} because this also reduces the average polarity of the reaction medium.

The representative temperature dependence of the LE emission decay of P4C in aqueous solution at f_{TBA} = 0.5 is shown in Figure 5, where decays collected at ~278 and 318 K are shown along with biexponential fit parameters. Data at further higher temperatures are not shown in this figure in order to avoid crowding, but fits through emission decays at three different temperatures (278, 318, and 373 K) are presented in Figure S5 (Supporting Information). Both the collected decays and fit parameters shown in these figures clearly suggest that the reaction time constant becomes faster as the temperature is increased. In fact, the reaction time constant at 373 K (~60 ps) is approximately two times and four times faster than those measured, respectively, at 318 and 278 K in this solution with f_{TBA} = 0.5. Temperature-induced enhancement of the reaction rate constant (k_{rxn} = τ_{rxn}^{-1}) has also been found for other mixture compositions as well.

Next, the temperature dependences of the measured τ_{rxn} at various TBA mole fractions are presented in Figure 6, where the natural logarithm of the reaction rate constant is shown as a function of the inverse temperature. The logarithm of the reaction rate constant decreases monotonically with inverse temperature at all TBA mole fractions, indicating an Arrhenius-type temperature dependence. Subsequently, the mole-fraction-dependent average activation energy (ΔE_{act}) for the photoinduced LE → CT conversion reaction of P4C in aqueous solutions of TBA is obtained by fitting the measured rate constants to the Arrhenius equation,[65] $\ln[(k_{rxn}/s^{-1})] = \ln[(A/s^{-1})] - (\Delta E_{act}/RT)$, where the quantities A and R bear the traditional meanings. The lines going through the data points represent the linear fits. The average activation energies thus obtained at different mixture compositions are presented in Figure 7 as a function of TBA mole fraction. Our limited attempt to recalculate ΔE_{act} at a few TBA mole fractions corresponding to very dilute and concentrated solutions from temperature-dependent measurements of the reaction rate suggests that these ΔE_{act} are associated with a maximum uncertainty of ±10% of the reported values. Even though the number of data points is rather limited (particularly at the low TBA concentration end) and somewhat scattered, it is evident in Figure 7 that ΔE_{act} rises steeply with the TBA mole fraction in the very low concentration regime and then suddenly changes the slope to level off with further addition of TBA in the aqueous mixture. Interestingly, the value to which ΔE_{act} levels off is ~$6k_BT$, which is quite close to the value estimated from the room-temperature pure solvent data using a Kramer's-type analysis in the limit of no solvent dynamic effects.[39] Values of ΔE_{act} in the TBA-rich regime are separately shown in the inset in order to clearly denote the value of the f_{TBA} around which a sharp variation in the slope occurs. One of the important aspects of the data presented in Figure 7 is that the average activation energy,

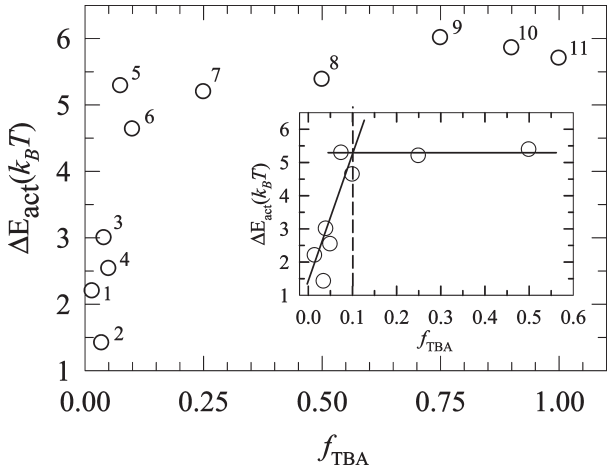

Figure 7. Mixture composition dependence of the average activation energy for the LE → CT conversion reaction of P4C in a water−TBA binary mixture. The number attached to each circle represents the serial number corresponding to a TBA mole fraction shown in Table S3 (Supporting Information). The maximum uncertainty associated with these ΔE_{act} is ±10% of the reported values. Note the abrupt change in slope for the mole fraction dependence of the activation energy. The inset shows more clearly the sudden change in slope as the mixture composition crosses the TBA mole fraction at which structural transition takes place. Solid and dashed lines are for visual guide. Note that the approximation of ΔE_{act} values by two straight lines is done to rather broadly describe the solution structural effects on the activation energy, and considering the scatter in the data, these two lines may not intersect exactly at f_{TBA} = 0.10 but should be close to that.

which has become as low as $\sim 1.5 k_B T$ at extremely dilute solutions due to very high polarity,[66−68] changes its slope of TBA concentration dependence at $f_{TBA} \approx 0.1$. Note that the average rotation rate of a dipolar solute also shows a sudden change in slope around this TBA concentration in aqueous solution.[11] This is the TBA mole fraction at which a transition occurs from a tetrahedral water-type network to a zigzag alcohol-like structure in solution. These data, however, do not indicate the presence of the expected minimum[69] in ΔE_{act} near $f_{TBA} \approx 0.04$. This may be due to the following reasons: (i) semiaccurate measurements of the mole-fraction-dependent reaction time constants due to the insufficient time resolution employed in the experiments and (ii) environmental effects being "averaged out" due to the short lifetime of the alcohol clusters formed at or around this mole fraction.

A juxtaposition of the heterogeneity aspects of (water + TBA) binary mixtures revealed by the present steady-state and time-resolved spectroscopic measurements against the solution structure suggested by the light-scattering[8,9,22,36] and SAXS measurements[5,35] led to the following interesting observation. While both the light- and X-ray-scattering experiments indicate growth of the correlation length (related to the concentration fluctuation and thus the distribution of TBA molecules in the system) with temperature and a nonmonotonic TBA mole fraction dependence showing a maximum at $f_{TBA} \approx 0.15$, the spectral (absorption) shift remains the largest at $f_{TBA} \approx 0.04$ in aqueous solution. Time-resolved fluorescence experiments, on the other hand, have indicated a change in the slope of the solution composition-dependent activation energy associated with a TICT reaction at $f_{TBA} \approx 0.10$. These contrasting results may be understood in the following manner. Because both compactness of solution structure due to inclusion of TBA in the water network and formation of clusters upon raising the temperature enhance chromophore−environment interactions via local density and polarity effects, respectively, the spectral shift becomes the largest at a particular composition where combined effects from these two solution aspects (local compactness and polarity) are maximized. Solution structural rigidity is known to be the highest at $f_{TBA} \approx 0.05$,[8,22] and scattering experiments[9,35] indicate clusters involving 2−4 TBA and 15−25 water molecules at this composition in this temperature range. The static dielectric constant at 298 K of the solution at this composition is only ~10% less than that of pure water ($\varepsilon_0^{water} \approx 80$).[15] Therefore, both the preservation of the three-dimensional water network and temperature-induced clustering at $f_{TBA} \approx 0.05$ then probably cause the maximum spectral shift of the dissolved chromophore, P4C. Further increase in TBA concentration leads to an increase in cluster size and growth of the correlation length, which eventually falls off with f_{TBA}, showing a maximum at $0.10 \leq f_{TBA} \leq 0.14$.[35] This sudden change in local environment is reflected in the abrupt change in slope for the composition dependence of the activation energy associated with the TICT reaction in P4C. Interestingly, solution compressibility increases and average polarity decreases at $f_{TBA} > 0.05$, regardless of the increase in either the TBA concentration or temperature.[15,22] The decrease in polarity is subsequently reflected in the blue shift of the spectrum. Because of the uncertainty (±10% of the reported value) associated with the estimated activation barrier (in solutions with $f_{TBA} \leq 0.05$), it cannot be confidently said that the data in Figure 7 indicate any minimum in ΔE_{act} with respect to TBA concentration as observed for the activation enthalpy change ($\Delta H^{\ddagger}$) associated with the solvolysis of tertiary butyl chloride in (water + TBA) mixtures.[70]

4. CONCLUSION

The work presented here indicates that the temperature-assisted aggregation of TBA molecules depends on the mixture composition, the extent of aggregation being the largest at a 0.04 TBA mole fraction, a concentration at which extreme changes in various thermodynamic properties are known to occur and maximization of hydrophobic effects are believed to take place. Temperature-dependent SANS experiments suggest clustering of a few tens of TBA molecules (or even larger) at this alcohol concentration and at T(K) ≈ 353. The effects of such an aggregation are reflected in the largest absorption shift measured at this TBA mole fraction. Fluorescence emission, however, does not show any red shift, and this has been attributed to the relatively shorter lifetime of the clusters than the average residence time of the chromophore in its excited state. Even though the measured reaction times for the intramolecular charge-transfer process in the dissolved chromophore do not show the effects of maximization of hydrophobic effects, the structural transition at TBA mole fraction ≈ 0.10 is well-indicated in the experimentally measured mole-fraction-dependent average activation energy. In addition, the measured activation energy at higher alcohol concentrations, where the solution structure is more "homogenized", agrees well with the value estimated earlier using the room-temperature solvent data. Note further that measurements of solution heterogeneity by employing SANS or other experimental techniques have not been performed yet over the composition range considered here. The work presented here, therefore, is expected to stimulate

further experimental and computer simulation studies of temperature effects on the heterogeneity at various alcohol concentrations in binary mixtures of TBA and water, in ternary mixtures containing a third component, and in other polar binary mixtures.[71]

■ ASSOCIATED CONTENT

Supporting Information. Table containing numerical values for the absorption peak frequency and spectral width of P4C in aqueous solutions of TBA at different solution compositions and temperatures, temperature-dependent absorption and emission spectra, temperature-dependent shift at higher TBA mole fractions (TBA-rich region), comparison between single and biexponential fits to the emission intensity decay, and fits to the collected decays at three representative temperatures. This material is available free of charge via the Internet at http://pubs.acs.org.

■ AUTHOR INFORMATION

Corresponding Author
*E-mail: ranjit@bose.res.in.

■ ACKNOWLEDGMENT

We sincerely thank Professor M. Maroncelli for encouragement and generous support. We thank an anonymous reviewer for bringing to our attention ref 35. It is a pleasure to acknowledge the assistance received from Dr. T. Pradhan at the initial stage of this work. H.G. thanks the Vice-Chancellor, Aliah University, West Bengal, for encouragement.

■ REFERENCES

(1) Dixit, S.; Crain, J.; Poon, W. C. K.; Finney, J. L.; Soper, A. K. *Nature* **2002**, *416*, 829.
(2) (a) Soper, A. K.; Finney, J. L. *Phys. Rev. Lett.* **1993**, *71*, 4346. (b) Bowron, D. T.; Finney, J. L.; Soper, A. K. *J. Phys. Chem. B* **1998**, *102*, 3551.
(3) Bowron, D. T.; Moreno, S. D. *J. Phys. Chem. B* **2005**, *109*, 16210.
(4) Yoshida, K.; Yamaguchi, T. *Z. Naturforsch., A: Phys. Sci.* **2001**, *56*, 529.
(5) Nishikawa, K.; Kodera, Y.; Iijima, T. *J. Phys. Chem.* **1987**, *91*, 3694.
(6) Koga, Y. *Chem. Phys. Lett.* **1984**, *111*, 176.
(7) Iwasaki, K.; Fujiyama, T. *J. Phys. Chem.* **1977**, *81*, 1908.
(8) Euliss, G. W.; Sorensen, C. M. *J. Chem. Phys.* **1984**, *80*, 4767.
(9) Iwasaki, K.; Fujiyama, T. *J. Phys. Chem.* **1979**, *83*, 463.
(10) Pradhan, T.; Ghoshal, P.; Biswas, R. *J. Phys. Chem. A* **2008**, *112*, 915.
(11) Pradhan, T.; Ghoshal, P.; Biswas, R. *J. Chem. Sci.* **2008**, *120*, 275.
(12) Brai, M.; Kaatze, U. *J. Phys. Chem.* **1992**, *96*, 8946.
(13) Murthy, S. S. N. *J. Phys. Chem. A* **1999**, *103*, 7927.
(14) Wojtkow, D.; Czarnecki, M. *J. Phys. Chem. A* **2005**, *109*, 8218.
(15) Kaatze, U.; Schumacher, A.; Pottel, R. *Ber. Bunsen-Ges. Phys. Chem.* **1991**, *95*, 585.
(16) Franks, F., Ed. *Water Science Reviews*; Cambridge University Press: Cambridge, U.K., 1985; Vol. 1.
(17) Bowron, D. T.; Finney, J. L. *J. Phys. Chem. B* **2007**, *111*, 9838.
(18) (a) Omelyan, I.; Kovalenko, A.; Hirata, F. *J. Theor. Comput. Chem.* **2003**, *2*, 193. (b) Yoshida, K.; Yamaguchi, T.; Kovalenko, A.; Hirata, F. *J. Phys. Chem. B* **2002**, *106*, 5042.
(19) Huang, D. M.; Chandler, D. *Proc. Natl. Acad. Sci. U.S.A.* **2000**, *97*, 8324.
(20) Tanaka, H.; Nakanishi, K.; Touhara, H. *J. Chem. Phys.* **1984**, *81*, 4065.
(21) Onori, G.; Santucci, A. *J. Mol. Liq.* **1996**, *69*, 161.
(22) Bender, T. M.; Pecora, R. *J. Phys. Chem.* **1986**, *90*, 1700.
(23) Rick, S. W.; Berne, B. J. *J. Phys. Chem. B* **1997**, *101*, 10488.
(24) Wallqvist, A. *J. Phys. Chem.* **1991**, *95*, 8921.
(25) Jungwirth, P.; Zahradink, R. *Chem. Phys. Lett.* **1994**, *217*, 319.
(26) Kiselev, M.; Ivlev, D.; Puhovski, Y.; Kerdcharoen, T. *Chem. Phys. Lett.* **2003**, *379*, 581.
(27) Wallqvist, A. *Chem. Phys. Lett.* **1991**, *182*, 237.
(28) Calandrini, V.; Deriu, A.; Onori, G.; Lechner, R. E.; Pieper, J. *J. Chem. Phys.* **2004**, *120*, 4759.
(29) Raschke, T. M.; Tsai, J.; Levitt, M. *Proc. Natl. Acad. Sci. U.S.A.* **2001**, *98*, 5965.
(30) Hone, D. W.; Pincus, P. A. *Europhys. Lett.* **2006**, *76*, 952.
(31) Paschek, D. *J. Chem. Phys.* **2004**, *120*, 6674.
(32) Mancera, R. L.; Buckingham, A. D.; Skipper, N. T. *J. Chem. Soc., Faraday Trans.* **1997**, *93*, 2263.
(33) Mancera, R. L.; Buckingham, A. D. *Chem. Phys. Lett.* **1995**, *234*, 296.
(34) Has, M.; Ludemann, H.-D. *Prog. Colloid Polym. Sci.* **1991**, *84*, 283.
(35) Nishikawa, K.; Hatashi, H.; Ijima, T. *J. Phys. Chem.* **1989**, *93*, 6559.
(36) Ito, N.; Kato, T.; Fujiyama, T. *Bull. Chem. Soc. Jpn.* **1981**, *54*, 2573.
(37) Sharp, K. A.; Nicholis, A.; Fine, R. F.; Honig, B. A. *Science* **1991**, *252*, 106.
(38) Sato, T.; Chiba, A.; Nozaki, R. *J. Chem. Phys.* **1999**, *110*, 2508.
(39) Dahl, K.; Biswas, R.; Ito, N.; Maroncelli, M. *J. Phys. Chem. B* **2005**, *109*, 1563.
(40) Pradhan, T.; Gazi, H. A. R.; Biswas, R. *J. Chem. Sci.* **2010**, *122*, 481.
(41) Pradhan, T.; Biswas, R. *J. Phys. Chem. A* **2007**, *111*, 11524.
(42) Pradhan, T.; Biswas, R. *J. Solution Chem.* **2009**, *38*, 517.
(43) Pradhan, T.; Gazi, H. A. R.; Biswas, R. *J. Chem. Phys.* **2009**, *131*, 054507.
(44) Pradhan, T.; Biswas, R. *J. Phys. Chem. A* **2007**, *111*, 11514.
(45) Grabowski, Z. R.; Rotkiewicz, K.; Rettig, W. *Chem. Rev.* **2003**, *103*, 3899.
(46) Lippert, E.; Rettig, W.; Bonačić-Koutecký, V.; Heisel, F.; Miehe, J. A. *Adv. Chem. Phys.* **1987**, *68*, 1.
(47) Zachariasse, K. A.; Grobys, M.; von der Haar, T.; Hebecker, A.; Il'ichev, Y. V.; Jiang, Y. B.; Morawski, O.; Kuhnle, W. *J. Photochem. Photobiol., A* **1996**, *102*, 59.
(48) Zachariasse, K. A. *Chem. Phys. Lett.* **2000**, *320*, 8.
(49) Rettig, W. *J. Luminesc.* **1980**, *26*, 21.
(50) Rettig, W. *J. Phys. Chem.* **1982**, *86*, 1970.
(51) Biswas, R.; Lewis, J. E.; Maroncelli, M. *Chem. Phys. Lett.* **1999**, *310*, 485.
(52) Lewis, J. E.; Biswas, R.; Robinson, A. G.; Maroncelli, M. *J. Phys. Chem. B* **2001**, *105*, 3306.
(53) Lakowicz, J. R. *Principles of Fluorescence Spectroscopy*, 2nd ed.; Kluwer Academic/ Plenum Publishers: New York, 1999.
(54) Horng, M. L.; Gardecki, J. A.; Papazyan, A.; Maroncelli, M. *J. Phys. Chem.* **1995**, *99*, 17311.
(55) Maroncelli, M.; Fleming, G. R. *J. Chem. Phys.* **1987**, *86*, 6221.
(56) Chapman, C. F.; Maroncelli, M. *J. Phys. Chem.* **1991**, *95*, 9095.
(57) Kusalik, P. G.; Lyubertsev, A. P.; Bergman, D. L.; Laksonen, A. *J. Phys. Chem. B* **2000**, *104*, 9533.
(58) Buchner, R.; Barthel, J.; Stauber, J. *Chem. Phys. Lett.* **1999**, *306*, 57.
(59) Ronne, C.; Thrane, L.; Astrand, P.-O.; Wallqvist, A.; Mikkelsen, K. V.; Keiding, S. O. *J. Chem. Phys.* **1997**, *107*, 5319.
(60) Petrowosky, M.; Frech, R. *J. Phys. Chem. B* **2009**, *113*, 16118.
(61) Reference 60 contains temperature-dependent dielectric constant values for several monohydroxy alcohols but not for tertiary butanol (TBA). It is assumed that the dielectric constant of TBA would

decerase with an increase in temperature, as has been found in ref 60 for other alcohols.

(62) Richert, R.; Heuer, A. *Macromolecules* **1997**, *30*, 4038.

(63) Arzhantsev, S.; Jin, H.; Ito, N.; Maroncelli, M. *Chem. Phys. Lett.* **2005**, *417*, 524.

(64) Bevington, P. R. *Data Reduction and Error Analysis for the Physical Sciences*; McGraw-Hill: New York, 1969.

(65) Atkins, P. W. *Physical Chemistry*; Oxford University Press: Oxford, U.K., 1994.

(66) Hicks, J.; Vandersall, M.; Babarogic, Z.; Eisenthal, K. B. *Chem. Phys. Lett.* **1985**, *116*, 18.

(67) Hicks, J.; Vandersall, M. T.; Sitzmann, E. V.; Eisenthal, K. B. *Chem. Phys. Lett.* **1987**, *135*, 413.

(68) Nag, A.; Kundu, T.; Bhattacharyya, K. *Chem. Phys. Lett.* **1989**, *160*, 257.

(69) A minimum in the mole-fraction-dependent average activation energy at $f_{TBA} \approx 0.04$ is "expected" according to the polarity effects described in refs 66−68 because the polarity of the microscopic polar domain is supposed to be the maximum at this TBA mole fraction.

(70) Robertson, R. E.; Sugamori, S. E. *J. Am. Chem. Soc.* **1969**, *91*, 7254.

(71) Roy, S.; Banerjee, S.; Biyani, N.; Jana, B.; Bagchi, B. *J. Phys. Chem. B* **2011**, *115*, 685.